2011 International Conference on Electrical Engineering and Informatics
17-19 July 2011, Bandung, Indonesia

A Comparative Study of Electromagnetic Generator via Finite Element Element Analysis

Zuraini Dahari[#1], Wong Chin Chye[#1], Othman Sidek*[2], Muhammad Azman Miskam *[2],

[#] *School of Electrical & Electronic Engineering, Universiti Sains Malaysia, 14300 Nibong Tebal, Pulau Pinang,* Malaysia

zuraini@eng.usm.my, wongchnchy@yahoo.com

* *Collaborative Microelectronic Design Excellence Centre*
Universiti Sains Malaysia, Engineering Campus, 14300 Nibong Tebal
Sri Ampangan, Pulau Pinang, Malaysia

othman@cedec.usm.my, azman@cedec.usm.my

Abstract— **Energy scavenging from ambient sources is an attractive alternative to batteries because of an almost unlimited lifetime and is environmentally safe. Environmental vibration is a particularly attractive energy source because of its abundance, and several scavenging techniques such as piezoelectric, electrostatic and electromagnetic (EM) transduction. Since it is quite easy to keep a strong magnetic field with a permanent magnet, electromagnetic vibration-power generators are preferred in many applications. This paper presents a comparative study of electromagnetic generator via Finite Element Analysis (FEA). It involves the investigation of the magnetic behaviours for several configurations of electromagnetic generator. The configuration varies in terms of types of magnet and the arrangement of the magnet. Finite element models are developed and further analyzed via ANSYS software. Analyses are conducted prior to investigate the magnetic behaviours of the electromagnetic generator such as the flux lines, the magnetic flux density and also the electromotive force (emf) produced.**

Keywords— **Comparative analysis, electromagnetic microgenerator, finite element analyses.**

I. Introduction

The most recent trend has seen researchers working and developing on renewable energy sources such as solar, thermal, vibration [1], and acoustic [2]. These sources are believed to be clean and have theoretically infinite life compared to batteries. These ambient energy sources are attractive alternative energy solution for implantable and embedded micro-systems that operate and depend on their initial energy supply [3]. Energy can be extracted from the vibration sources via mechanical-to electrical power generator by using piezoelectric, electrostatic and electromagnetic principles.

Ordinary power generation from environment include solar (outdoor/indoor), vibration, acoustic noise, daily temperature variation, and temperature gradient while energy scavenging from chemical fuel are nuclear source, batteries (lithium), combustion (micro-engine), and fuel cells (methanol) [3]. An overview and on-going research works on vibration based electromagnetic micro generator have been presented in our previous work [3]. Several important parameters such as the shape, types of magnet, spring and coil used in designing electromagnetic micro generator and also power processing circuit are discussed. Different designs of micro generator with different resonant frequency for different environment and application are also discussed

Generally, the electromagnetic generator makes use of Faraday’s law of induction [1, 4]. The vibration is used to move a magnetic mass move relative to a coil or vice versa, thus inducing a voltage and cause a current flow in the close circuit. This paper presents a comparative study of electromagnetic generator via Finite Element Analysis (FEA). Investigations on magnetic behaviours of different configurations of electromagnetic generators are conducted via FEA.

According to P.Glynne-Jones and *et. al.*, two configurations as shown in Fig. 1 was studied. The first configuration consists of two magnets, Fig. 1(a) while the second configuration, Fig 1(b) consists of four magnets [5]. Neodymium Iron Boron magnet was used in his design. First configuration electromagnetic generator is capable of producing useful level of power, however the output voltage is considered too low for practical application. Meanwhile, the second configuration is able to generating useful power and voltage levels from ambient vibrations. An average power of 157 µW is obtained when a similar device described mounted on the engine block of a car [5].

This paper will investigate different configurations of electromagnetic generator via FEA. It involves the investigation of the magnetic behaviours for several configurations of electromagnetic generator. The configuration varies in terms of types of permanent magnet and also the arrangement of the magnets. Finite element models are developed and further analysed via ANSYS software. Through these results, the emf output of each configuration can be predicted. This study serves as a

978-1-4577-0751-3/11/$26.00 ©2011 IEEE

preliminary effort for further research work in designing an electromagnetic generator.

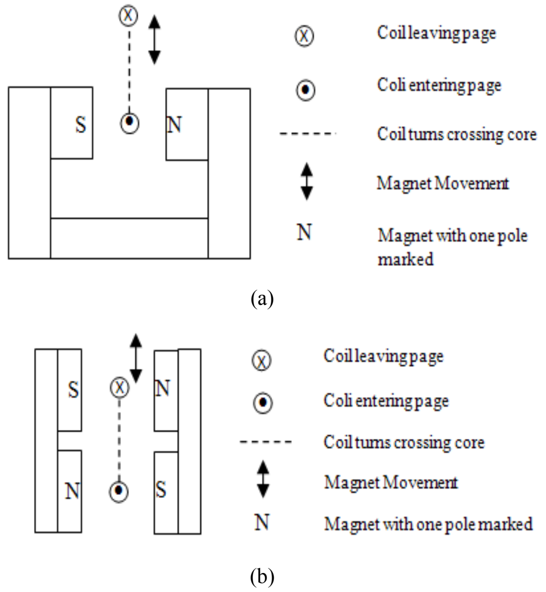

Fig. 1 Configurations studied by P.Glynne-Jones and *et. al.[5].*

II. BASIC THEORY

A. Basic Theory of Electromagnetic Generator

Generally, electromagnetic resonant generator comprises of permanent magnet, spring and coil. This generator can also be referred as velocity damped resonant generator (VDRG) as the damping force is proportional to the proof mass internal velocity [6]. The simplified mechanical model of VDRG used for analysis is shown in Fig. 2. The mass of the vibration source is assumed to be much greater than the mass of the seismic mass in the generator and the vibration source should be infinite source of power [7].

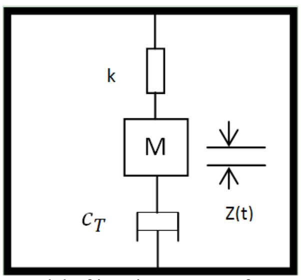

Fig. 2 Model of inertia generator for analysis.

This resonant generator can be represented by a second-order spring mass damper differential equation with base excitation which describes the movement of the mass with respect to the generator housing [7]. If the base or housing of the generator is excited with a displacement $y(t) = Ysin(\omega t)$, it will vibrate out of phase with the mass at resonance causing a net displacement between the housing and the mass, this relative motion of the mass with respect to the base is $z(t)$, then the differential equation of motion is:

$$m\ddot{z}(t) + c_T\dot{z}(t) + kz(t) = -m\ddot{y}(t) \quad (1)$$

Where m is mass of seismic mass, c_T is damping coefficient, k is spring constant. A comprehensive analyses derivation can be referred in details in research work conducted by Mitcheson and *et. al*.[4].

In the case of electromagnetic transducer, the force on a wire terminated with a load resistance R, moving through a magnetic field is given by,

$$F = \frac{(Bl)^2}{R}v \quad (4)$$

Where B is magnetic flux density, l is length of wire, R is load resistance and v is velocity of coil. Since damping force is proportional to velocity, the damping coefficient as below:

$$c_T \approx \frac{(Bl)^2}{R} \quad (5)$$

Assume that parasitic loss mechanism such as air damping can be neglected [7]. This shows that the damping factor for the device can be managed by changing the electrical load resistance, R to obtain optimal performance for application[7].

B. Faraday's Law of Induction

Faraday's law of induction state that the induced electromotive force (EMF) in any closed circuit is equal to the time rate of change of the magnetic flux through the circuit [8]. This law makes use of the magnetic flux ф through an integral surface area, *ds*. Fig. 3 shows a closed rectangular loop of wire in xy-plane. The coil moves along the x-direction at velocity v, where $v = \frac{dx}{dt}$. The rectangular loop has width *w* in x-direction while length *l* in y-direction. The magnetic field on the right-hand side (RHS) is *B(x+w/2)* and on the left-hand side (LHS) is *B(x-w/2)*, where magnetic field *B(x)* is a time independent but spatially varying field pointing along z-axis.

$$\Phi = l\int_{x-w/2}^{x+w/2} B(x)dx \quad (6)$$

The sign of flux is determined by the direction of the normal to the surface points. The sign is negative if we take the normal to the surface as pointing in the same direction as the B-field of induced current. Since the induced electromotive force is the time derivative of the flux, thus

$$emf = \frac{d\Phi}{dt} = (-)vl\left[B\left(x + \frac{w}{2}\right) - B(x - \frac{w}{2})\right] \quad (7)$$

Where $v = \frac{dx}{dt}$. If a coil that consists of N loops, then the total induced emf would be N times,

$$emf, \varepsilon = -N\frac{d\Phi}{dt} = NB_{net}lv \quad (8)$$

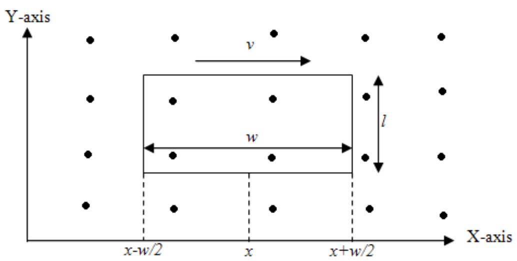

Fig. 3 A rectangular wire loop moving through magnetic field B with velocity *v* along the x-axis.

III. Electromagnetic Generator Design

A. Generator Design Overview

The typical electromagnetic microgenerator consists of cantilever, permanent magnets and coils. In this work, the proposed design comprises of a stainless steel cantilever, neodymium iron boron (NdFeB) magnets, copper coils and permalloy. Two high flux density NdFeB magnets were bonded with glue on the top and bottom surface of the end of cantilever while the other end of cantilever was fixed as shown in Fig. 4.

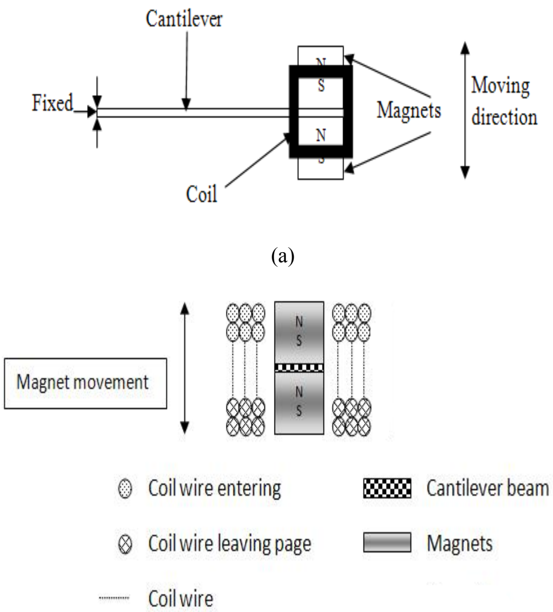

(a)

(b)

Fig. 4 Model of microgenerator (a) side view, (b) cross section view.

Table I list out the dimension for each component used in the proposed design. Initially, the coil has a rectangle shape placed at both side of the magnets as in Fig. 4(a). Copper coils are chosen as it has better conductivity and more cost-effective.

TABLE I
Dimension of Component on the Microgenerator

Component	**Material**	**Dimension (*w* x *h* x *d*) (mm)**
Cantilever	Stainless steel	45 x 10 x 0.5
Magnets	Neodymium iron boron (NdFeB)	10 x 10 x 10
Coils	Copper	10 x 30 x 5

B. Finite Element Analysis

The design was modelled in detail FEA tool in order to study the magnetic behaviours. A specific design is selected to investigate the magnetic behaviours of an electromagnetic generator design for different types of permanent magnets, as in Fig. 5. The finite element model for the design is developed using ANSYS software and analysed. The analyses were conducted for three types of PM, which are a ferrited magnet (Ceramic magnet), samarium-cobalt (SmCo) and neodymium-iron-boron (NdFeB).

NdFeB and SmCo have higher coercivity compare to Ceramic magnet which are 840 kA/m, 600 kA/m and 259 kA/m, respectively. However, the maximum service temperature for ceramic magnet is highest among these types of magnets compare to SmCo and NdFeB, such that 400 °C, 250 °C and 150 °C, respectively [9]. If higher temperature operation environment is required, then SmCo can be considered with moderate coercivity.

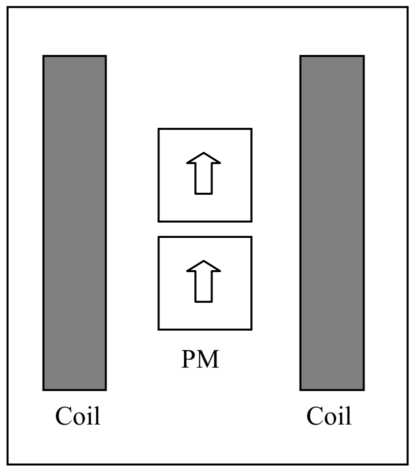

Fig. 5 The base model of electromagnetic generator

These three models for different type of PMs were analysed to study on the magnetic behaviours in each case. In order to extract the magnetic flux density of magnets in the models, reference paths were plotted along the copper coil to extract the magnetic flux density value. The simulation results of the magnetic flux lines and reference paths are demonstrated in Fig. 6.

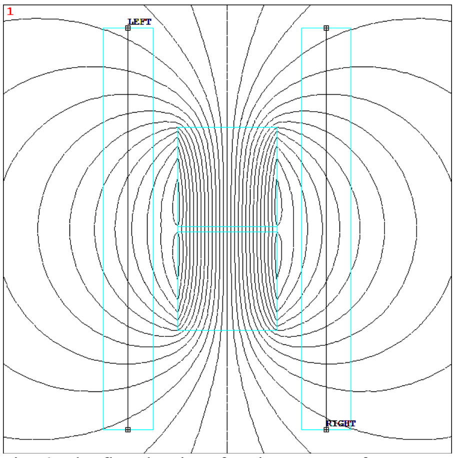

Fig. 6 The flux density of various types of magnets.

Fig. 7 shows the contour plot of flux density for three configurations. The values of the flux density for each PMs are illustrated beside the contour plot for the three types of magnets.

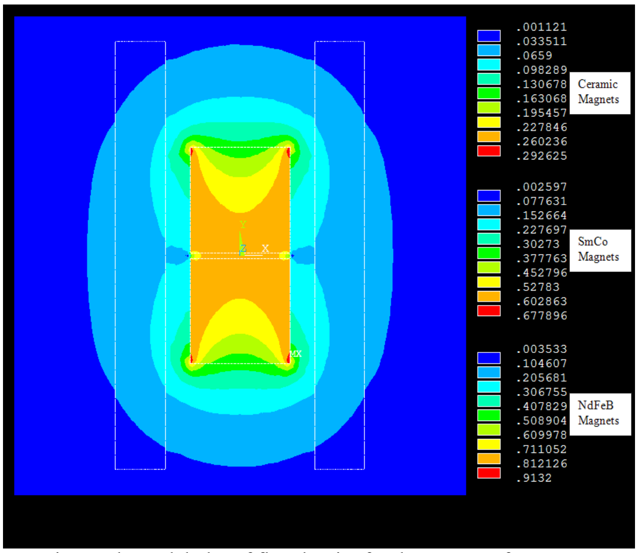

Fig. 7 The nodal plot of flux density for three types of magnets.

Since the B_x component is perpendicular to area of the coil, it contributes to the emf generation, hence we focused on the B_x component. The B_x values along the reference path were extracted from the analyses conducted. Fig. 8 illustrates the magnetic flux density along the copper coil for three different types of magnets.

As expected, NdFeB magnet gives the higher peak density on the coil, 0.1518 T while SmCo magnet gives 0.1118 T follows by ceramic magnet that reports 0.0483 T. Obviously, the magnet with higher coercivity is able to produce higher magnetic flux density compared to lower coercivity magnets.

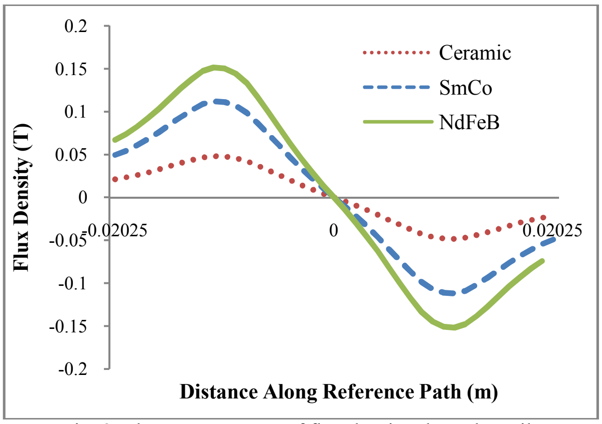

Fig. 8 The B_x component of flux density along the coil.

The next analyses involved the investigations on different arrangement of magnets, as in Fig. 9. NdFeB was chosen as the reference magnet and different arrangements of magnets were simulated. Configuration I consists of two axially magnetized PMs, whereas the second configuration consists of single PM, as in Fig. 9(a) and (b). The third configuration consists of two horizontally magnetized PMs in the same direction and the fourth configuration comprises of two PMs magnetized in opposite direction, Fig. 9(c) and (d). The magnetic flux density for the above mentioned configurations were shown in Fig. 10.

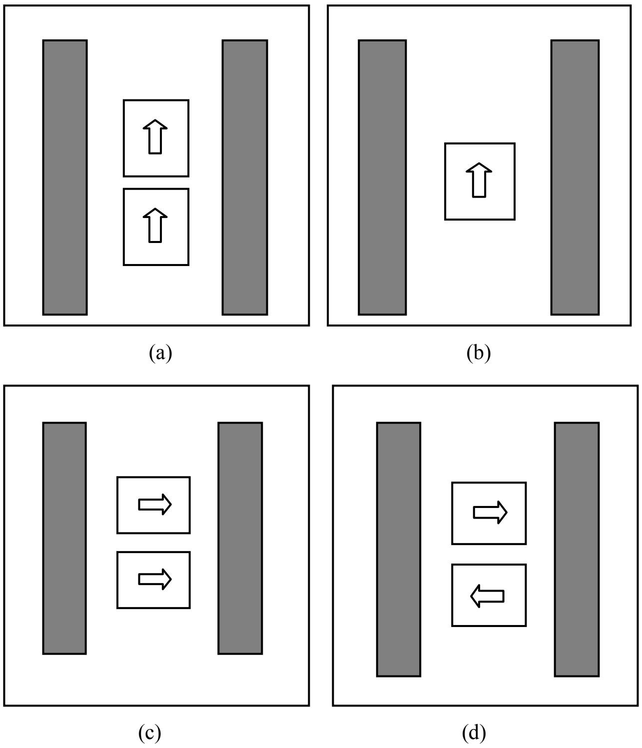

Fig. 9 Modeling of cross sectional magnets with different arrangement in ANSYS (a) Configuration I, (b) Configuration II, (c) Configuration III , (d) Configuration IV.

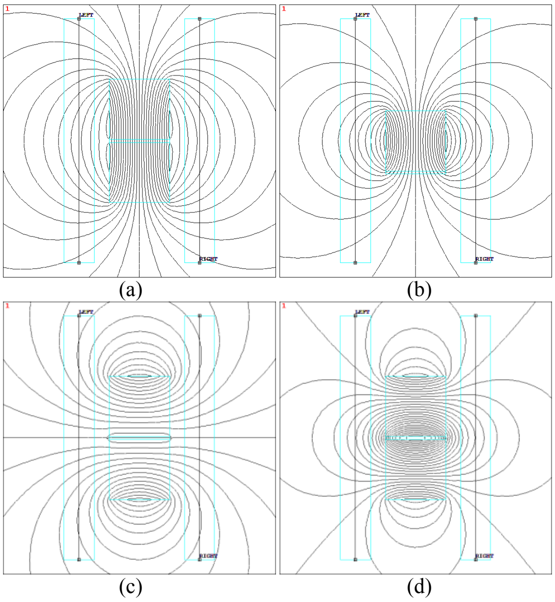

(a) (b)

(c) (d)

Fig. 10 The flux density of above mentioned configurations (a) Configuration I, (b) Configuration II, (c) Configuration III , (d) Configuration IV.

Again, the magnetic flux density among four configurations were studied by referring to the reference path of the right hand side of the coil. Fig. 11 demonstrates the comparison of flux density values for the four configurations. Configuration I, II, and IV demonstrate maximum flux density values of 0.1518 T, 0.1090 T, and 0.1633 T respectively. Meanwhile Configuration III showed the peak flux density of 0.1649 T and the characteristic of symmetric.

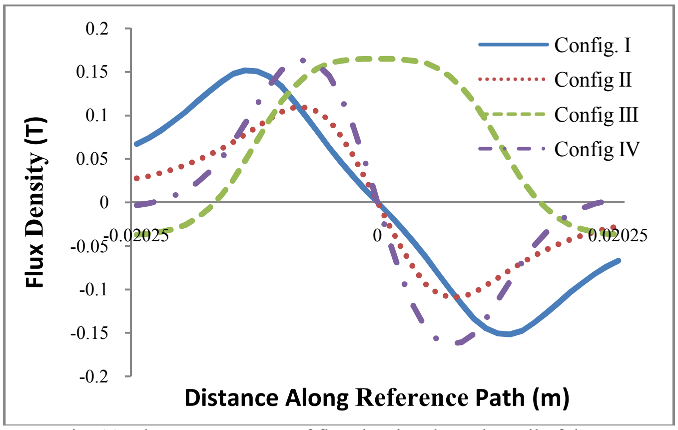

Fig. 11 The B_x component of flux density along the coil of three configurations.

The next task is to study on the generated emf in these cases. Fig. 12 shows the modelling of cross section of microgenerator for four configurations in the FEA. In the simulation performed, the magnets are moved from -10 mm to +10 mm divided into 20 sections in order to simulate the situation where the magnets vibrate. The magnets are moved from one position to another position in order to obtain the magnetic value density value for the coils. During each movement, the magnetic flux density value for each of the node of coil is recorded in a table. The average flux density values are obtained from the element table and extracted to calculate the emf. The velocity of the magnets is derived from the mathematical equation as the movement of the magnets can be modelled in the mathematical equation of a cosine function.

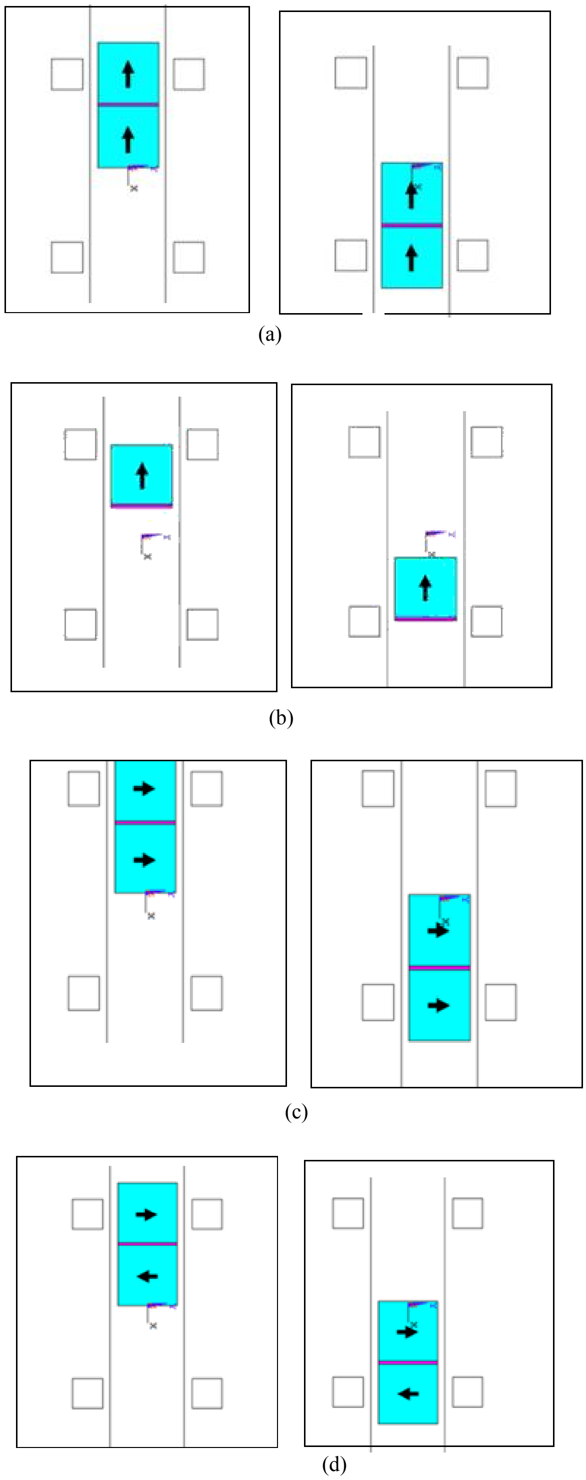

(a)

(b)

(c)

(d)

Fig. 12 The modelling of initial (left) and final (right) position of the magnets for (a) Configuration I, (b) Configuration II, (c) Configuration III, (d) Configuration IV.

Fig. 13 shows the simulated emf for various configurations. As can be seen from the graph, Configuration I and II produced harmonic waveform while the other two configurations demonstrated distorted waveforms. Configuration I shows the highest peak voltage as 4.44 mV while Configuration II illustrates a voltage at 1.9 mV.

In order to obtain a harmonic waveform, $\left[B\left(x+\frac{w}{2}\right)-B(x-\frac{w}{2})\right]$ must be a symmetric waveform, so that the multiplying between velocity and flux density creates proper harmonic waveform. For harmonic motion of pendulum, the velocity of object is highest when the displacement is equal to origin. In this case, the velocity of magnet is highest when it reaches the origin. Thus, we get peak voltage when it reaches the origin. As the magnet go through from initial to the final position, a peak voltage is produced while a similar peak voltage but different polarity is produced when it go through the opposite direction. Then, we obtain a proper harmonic waveform of emf.

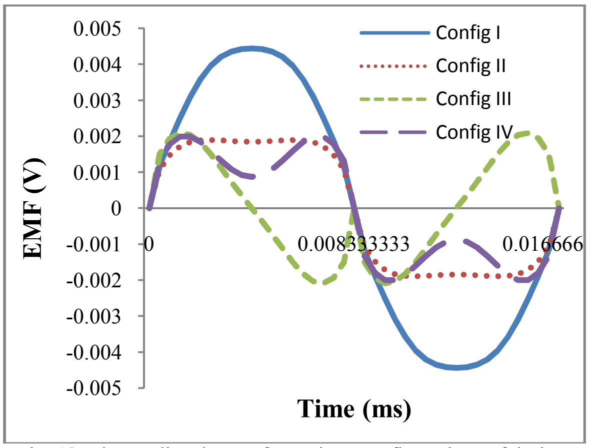

Fig. 13 The predicted EMF for various configurations of design.

Based on the FEA results, we can conclude that Configuration I generated higher emf compared to the other three configurations. Therefore, the arrangement is the most suitable configuration to be applied for the design of electromagnetic generator.

IV. Conclusions

This paper has presented the comparative analysis on electromagnetic generator designs via finite element analysis. The main objective of this study is to investigate the impact of various types of magnets and also for different configurations of magnets in the design. In terms of types of permanent magnet, NdFeB produced the highest magnetic flux density compared to the other two magnets, which are SmCo and ceramic magnet. Four different configurations are simulated and analysed via finite element analysis. The results are compared in terms of the magnetic flux density value and the emf produced. Based on the results, it demonstrated that the arrangement in Configuration I and II produced less distorted harmonic waveform. Configuration I demonstrated the highest emf, which is the desirable characteristic in designing electromagnetic microgenerator. In overall, the results showed that stronger magnet produced better electromotive force and the arrangement of the magnet also contribute to the performance of the electromagnetic generator. Hence, the arrangement can be utilised to produce steady power supply to power up certain micro system.

Acknowledgment

The author acknowledge the financial support from the Universiti Sains Malaysia's Short Term Grant, 304/PELECT/ 6039027 and Universiti Sains Malaysia Fellowship .

References

[1] Cian ´O Math´una, Terence O'Donnell, Rafael V. Martinez-Catala, James Rohan, and B. O'Flynn, "Energy scavenging for long-term deployable wireless sensor networks.," *Talanta,* vol. 75, pp. 613–623, 2008.

[2] T. Lai, C. Huang, and C. Tsou, "Design and Fabrication of Acoustic Wave Actuated Microgenerator for Portable Electronic Devices," in *DTIP of MEMS & MOEMS 9-11 April 2008*.

[3] Wong Chin Chye, Zuraini Dahari, Othman Sidek, and M. A. Miskam, "Electromagnetic Micro Power Generator - A Comprehensive Survey," in *2010 IEEE SYMPOSIUM ON INDUSTRIAL ELECTRONICS & APPLICATIONS* Penang, Malaysia, 2010.

[4] S. M. Paul D. Mitcheson, IEEE, , S. M. Tim C. Green, IEEE, , M. Eric M. Yeatman, IEEE, , and M. Andrew S. Holmes, IEEE, "Architectures for Vibration-Driven Micropower Generators," *Journal of Microelectromechanical Systems,* vol. VOL. 13, , JUNE 2004.

[5] P. Glynne-Jones, M.J. Tudor, and N. M. W. S.P. Beeby, "An electromagnetic, vibration-powered generator for intelligent sensor systems," *Sensors and Actuators A,* vol. 110, pp. 344–349, 2004.

[6] P. D. Mitcheson, T. C. Green, and E. M. Yeatman, "Power Processing Circuits for MEMS Inertial Energy Scavengers " in *DTIP of MEMS & MOEMS*, Stresa, Italy, 26-28 April 2006.

[7] C. B. Williams and R. B. Yates, "Analysis of A Micro-electric Generator for Microsystems," in *The 8th International Conference on Solid-State Sensors and Actuators, and Eurosensors IX*. vol. 52, Issues 1-3 Stockholm, Sweden, 1995, pp. 8-11.

[8] M. N. O. Sadiku, *Elements of Electromagnetics*, Fourth ed.: New York (USA)/Oxford (UK): Oxford University Press, 2007.

[9] E. P. Furlani, "Permanent Magnet and Electromechanical Devices," I. Mayergoyz, Ed.: Academic Press, 2001, p. 39.